



ORIGINAL ARTICLE

# Structural analysis of the peptides temporin-Ra and temporin-Rb and interactions with model membranes

José L. S. Lopes<sup>1</sup>  · Caio C. F. Araujo<sup>2</sup>  · Rogério C. Neves<sup>3</sup>  · Jochen Bürck<sup>4</sup>  · Sheila G. Couto<sup>5</sup> 

Received: 8 April 2022 / Revised: 27 July 2022 / Accepted: 31 July 2022 / Published online: 17 August 2022  
 © European Biophysical Societies' Association 2022

## Abstract

The skin of amphibians is widely exploited as rich sources of membrane active peptides that differ in chain size, polypeptide net charge, secondary structure, target selectivity and toxicity. In this study, two small antimicrobial peptides, temporin-Ra and temporin-Rb, originally isolated from the skin of the European marsh frog (*Rana ridibunda*), described as active against pathogen bacteria and presenting low toxicity to eukaryotic cells were synthesized and had their physicochemical properties and mechanism of action investigated. The temporin peptides were examined in aqueous solution and in the presence of membrane models (lipid monolayers, micelles, lipid bilayers and vesicles). A combined approach of bioinformatics analyses, biological activity assays, surface pressure measurements, synchrotron radiation circular dichroism spectroscopy, and oriented circular dichroism spectroscopy were employed. Both peptides were able to adsorb at a lipid-air interface with a negative surface charge density, and efficiently disturb the lipid surface packing. A disorder-to-helix transition was observed on the secondary structure of both peptides when either in a non-polar environment or interacting with model membranes containing a negative net charge density. The binding of both temporin-Ra and temporin-Rb to membrane models is modulated by the presence of negatively charged lipids in the membrane. The amphipathic helix induced in temporin-Ra is oriented parallel to the membrane surface in negatively charged or in zwitterionic lipid bilayers, with no tendency for realignment after binding. Temporin-Rb, instead, assumes a  $\beta$ -sheet conformation when deposited into oriented stacked lipid bilayers. Due to their short size and simple composition, both peptides are quite attractive for the development of new classes of peptide-based anti-infective drugs.

**Keywords** Antimicrobial peptide · Oriented circular dichroism · Peptide–lipid interaction · Surface pressure · Synchrotron radiation circular dichroism spectroscopy · Temporin

## Abbreviations

AMPs Antimicrobial peptides  
 LUVs Large unilamellar vesicles  
 MIC Minimum inhibitory concentration

P/L Peptide-to-lipid molar ratio  
 RPC Reverse-phase chromatography  
 SRCD Synchrotron radiation circular dichroism  
 SR-OCD Synchrotron radiation oriented circular dichroism  
 POPG 1-Palmitoyl-2-oleoyl-sn-glycero-3-phosphoglycerol  
 POPC 1-Palmitoyl-2-oleoyl-sn-glycero-3-phosphocholine  
 S-state “Surface-bound” state  
 T-state Tilted state  
 I-state “Inserted” state  
 tRa Temporin-Ra  
 tRb Temporin-Rb

✉ Sheila G. Couto  
[gsheilac@gmail.com](mailto:gsheilac@gmail.com)

- <sup>1</sup> Instituto de Física, Universidade de São Paulo, São Paulo, SP 05080-900, Brazil
- <sup>2</sup> Faculdade de Medicina, Universidade Federal de Goiás, Goiânia, GO 74690-900, Brazil
- <sup>3</sup> Instituto de Patologia Tropical E Saúde Pública, Universidade Federal de Goiás, Goiânia, GO 74605050, Brazil
- <sup>4</sup> Institute of Biological Interfaces (IBG-2), Karlsruhe Institute of Technology (KIT), POB 3640, 76021 Karlsruhe, Germany
- <sup>5</sup> Instituto de Física, Universidade Federal de Goiás, Av. Esperança, s/n - Campus Samambaia, Goiânia, GO 74690-900, Brazil

## Introduction

Many different antimicrobial peptides (AMPs) (Varga et al. 2018; Kumar et al. 2018) have been isolated from the skin of amphibians. All these membrane-active molecules were shown to differ in their physico-chemical properties, such as chain size (Demori et al. 2019), toxicity (Zairi et al. 2009), net charge (Oger et al. 2019), adopted secondary structure (Helbing et al. 2019), and microorganism selectivity (Mishra et al. 2017). Some of the AMPs isolated from the frog skin have demonstrated elevated inhibitory action on different pathogenic organisms, including multidrug-resistant bacteria (Kim et al. 2018) and human infecting virus (Roy et al. 2019); and moreover, some have the ability to specifically attack some types of cancer cells (Hoskin and Ramamoorthy 2008). From the AMPs isolated from amphibians, the group of the temporins (term originally used to represent a group of small linear peptides isolated from the European red frog *Rana temporaria* (Mangoni et al. 2016)) is among the smallest  $\alpha$ -helix peptides found in nature (containing from 10 to 14 residues). The temporins are short linear peptides which are able to form amphipathic molecules presenting one positive side at neutral pH. The AMPs belonging to this group have been isolated from closely related species of frogs (Rinaldi et al. 2002) and presented biological activity dependent on the biophysical properties of the peptide and target membrane (Jenssen et al. 2006). Currently, there is an increasing interest on the group of the temporins because of their inhibitory action against a wide range of pathogens (Gram-positive bacteria, viruses, filamentous fungi and yeasts), and due to their low toxicity to mammalian cells. Thus, in the view of a global emergence of new drugs to fight against multiple resistant microorganisms, the characterization of such AMPs is also justified due to their low molecular weight and broad spectrum of action presented (Rinaldi and Conlon 2016).

Previous work performed by Asoodeh et al. (2012) (Asoodeh et al. 2012) has identified two novel AMPs from the temporins with a potential therapeutic application in the skin secretions of the marsh frog *Rana ridibunda*, named temporin-Ra (tRa) and temporin-Rb (tRb). The inhibitory action of these two peptides on *Escherichia coli*, *Streptococcus dysgalactiae*, *Klebsiella pneumoniae*, *Staphylococcus aureus* and *Streptococcus agalactiae* was demonstrated; however, the full mechanism of action used by each of these peptides is still unclear.

In this study, two synthetic versions of the antimicrobial peptides temporin-Ra and temporin-Rb were designed with their original amino acid sequences, composed of 14 and 12 amino acids, respectively. The structural behavior of both peptides in aqueous solution and in the presence

of model membranes (composed of Langmuir monolayers, oriented lipid bilayers, micelles, and vesicles) was examined by synchrotron radiation circular dichroism spectroscopy, synchrotron radiation oriented circular dichroism, and surface tension measurements. Both peptides were able to bind and effectively disturb the integrity of the membrane models with a negative surface charge density in aqueous solution, but also to bind oriented zwitterionic lipid bilayers. Although similar in sequence, the peptides presented slightly different structural behavior, and binding preferences during this interaction to model membranes.

## Materials and methods

### Peptide synthesis and purification

Temporin-Ra (FLKPLFNAALKLLP) and temporin-Rb (FLPVLAGVLSRA) were manually synthesized on Rink Amide resin by Fmoc solid-phase peptide synthesis (SPPS) as C-terminal amides. Fmoc-deblocking was carried out with 20% piperidine in dimethylformamide (DMF). Couplings were performed with the Fmoc-protected amino acids (2 equiv.), 2-(1H-7-azabenzotriazol-1-yl)-1,1,3,3-tetramethyl uranium hexafluorophosphate methanaminium (HATU), and N-ethyl-diisopropylamine (DIPEA) in a mixture 1/1 (vol/vol) of DMF/dichloromethane (DCM). At each step, the coupling/deprotection efficiency > 95% was monitored by Kaiser assay (Kaiser et al. 1970). Final peptide cleavage from the resin was achieved with a cleavage cocktail of trifluoroacetic acid (TFA)/triisopropylsilane (TIS)/H<sub>2</sub>O (94:2.5:2.5, v/v) for 2 h. The crude peptides were precipitated in cold diethyl ether, centrifuged at 3000 rpm for 5 min and lyophilized. Purification of the crude peptides was performed by reverse-phase chromatography (RPC) using an ÄKTA Purifier System (GE Healthcare) with an YMC-Pack Polymer C<sub>18</sub> column (250 × 4.6 mm, 6  $\mu$ m bead size, Waters, Germany) equilibrated with 0.1% (v/v) TFA/water. Elution was performed at a 1 ml/min flow rate using a linear gradient: from 5 to 95% of acetonitrile 90% in water containing 0.1% TFA over 30 min, with absorbance monitored at 220 nm. The purified peptides were analyzed by electrospray ionization mass spectrometry (ESI-MS), and peptide concentration was calculated by the absorbance at 205 nm method (Anthis and Clore 2013).

### Bioinformatics analyses

The sequence-based predictions of the secondary structure of tRa and tRb were performed with GOR4 (Combet et al. 2000) and Agadir (Muñoz and Serrano 1997) algorithms.

Helical wheel projections were performed with HeliQuest server (Gautier et al. 2008).

### Synchrotron radiation circular dichroism (SRCD) spectroscopy

The SRCD spectra of tRa and tRb (50  $\mu\text{M}$ ) in 10 mM sodium phosphate buffer (pH 7.4), and in 50 or 100% of trifluoroethanol (TFE) were collected at the AU-CD beamline of the ASTRID2 synchrotron facility (Aarhus, Denmark). The SRCD spectra were recorded from 170 to 280 nm in 1 nm intervals and 2 s dwell time, using a 0.01027 cm pathlength quartz cuvette (Hellma Scientific), as an average of 3 individual scans, at 25 °C. The peptides were also examined when incubated with membrane models composed of either 20 mM of sodium dodecyl sulfate (SDS), *N*-hexadecyl-*N*'-dimethyl-3-ammonio-1-propane-sulfonate (HPS), hexadecyltrimethylammonium bromide (CTAB) or large unilamellar vesicles of 1-palmitoyl-2-oleoyl-sn-glycero-3-phosphoglycerol (POPG), 1-palmitoyl-2-oleoyl-sn-glycero-3-phosphocholine (POPC) at a 1:50 peptide-to-lipid (P/L) molar ratio. Baselines for each sample (solution containing all the components, except the peptide) were measured in the same cell.

All SRCD data were processed with CDToolX software (Miles and Wallace 2018). The processing consisted of a calibration with camphorsulfonic acid, average of the three individual scans, subtraction of a corresponding baseline spectrum, smoothing with a Savitzky–Golay filter, zeroing over the range from 267 to 270 nm, and unit conversion to delta epsilon units using a mean residue weight of 121.9 and 112.9 and for tRa and tRb, respectively.

### Synchrotron radiation oriented circular dichroism (SR-OCD) spectroscopy

SR-OCD measurements were taken at the beamline UV-CD12 of the Karlsruhe Research Accelerator (KARA) from 260 to 180 nm, using 0.5 nm intervals, at 20 °C. The humidity and temperature within the sample cell were controlled with a capacitive relative humidity and temperature sensor (SHT 75, Sensirion, Zurich, Switzerland), fixed in the immediate vicinity of the sample (as described in Bürck et al. 2008) (Bürck et al. 2008). The spectra of lipid bilayers alone were measured at the same conditions, and subtracted from the corresponding sample spectra. For each P/L ratio at least two independently prepared samples were measured and averaged, and finally the data from a given series were normalized to have the same spectral magnitude at the long-wavelength minimum around 220 nm. Prior to the experiments at the beamline, preliminary oriented CD spectroscopy measurements had been taken at the IBG-2 (Karlsruhe Institute of Technology,

Germany) on a Jasco J-810 spectropolarimeter from 260 to 180 nm, using similar measurement parameters and averaging of spectra measured at eight positions of the plate (using a 45° rotation after each spectrum). However, spectra were quite noisy (and therefore are not shown here) and so it was decided to conduct the SR-OCD measurements, allowing for a better spectral quality.

Oriented lipid bilayers were prepared as described in Bürck et al. 2008 (Bürck et al. 2008), by co-dissolving each one of the lipids POPG or POPC (5 mg/ml) in a mixture of chloroform/methanol (1/1, v/v), and adding peptides (tRa or tRb) solubilized in methanol/TFE (95/5, v/v) at a peptide-to-lipid molar ratio of 1/50, 1/25, 1/18 and 1/12.5, and then vortexing to homogeneity. The peptide–lipid mixture (~30–50  $\mu\text{L}$ ) was deposited in a circular spot on the surface of a quartz glass Suprasil plate (Hellma), to promote the formation of the homogeneous films. Additionally, OCD samples of the temporin peptides in membranes of thinner hydrophobic thickness (C-8: 1,2-dioctanoyl-sn-glycero-3-phosphocholine (DOcPC); C-10: 1,2-didecanoyl-sn-glycero-3-phosphocholine (DDPC); and C-12: 1,2-dilauroyl-sn-glycero-3-phosphocholine (DLPC) were prepared according to the same procedure.

The plates were kept in a desiccator chamber under 3 mbar vacuum for 2 h to remove residual solvent and then maintained in a home-built CD chamber (Bürck et al. 2016) with controlled humidity (97.6% relative humidity, obtained with a saturated solution of  $\text{K}_2\text{SO}_4$ ) for 16 h at 20 °C, to promote the complete rehydration of the lipid on the plate and alignment of the peptides within the oriented lipid bilayers.

### Surface tension measurements

The surface properties of tRa and tRb (20  $\mu\text{M}$ ) in 10 mM sodium phosphate buffer (pH 7.4) were measured on a DeltaPi tensiometer (Kibron Finland), using a 15-well microplate. Peptides were injected to the aqueous subphase, and subsequent changes in surface pressure were monitored over 30 min, at 25 °C. Additionally, POPC and POPG monolayers with lateral packing density of 30 mM/m were formed on air/aqueous interface and after solvent evaporation tRa and tRb peptides (from 5 to 40  $\mu\text{M}$ ) were injected to the aqueous subphase, and the changes in surface pressure were registered for 120 min. Moreover, Langmuir monolayers of POPG with controlled lateral packing density (10–30 mM/m) were formed on top (air/aqueous interface) of a microplate well (filled with 1.2 ml of the aqueous solution). After solvent evaporation, each of the peptides (10  $\mu\text{M}$ ) was injected to the aqueous subphase and the subsequent changes in surface pressure due to the peptide adsorption were registered for 120 min.

## Hemolytic assay

The hemolysis of erythrocytes was determined spectrophotometrically by measuring the release of hemoglobin, based on the method described in Lopes et al. (Lopes et al. 2013). Briefly, tRa and tRb (500 µg/ml) in 10 mM Tris–HCl buffer (pH 7.4) containing 150 mM NaCl were incubated for 1 h at 37 °C with aliquots (100 µL) of a 1% (v/v) suspension of human erythrocytes in a two-fold serial dilutions (from 500 to 1.0 µg/ml). Subsequently, samples were centrifuged at 3000 × g for 2 min, the supernatant was collected and the hemolysis was determined measuring the absorbance of supernatant at 405 nm in a 96-well microplate reader. All experiments were carried out in triplicate, using a solution of 1% Triton X-100 as control of 100% lysis.

## Antibacterial activity

Determination of the minimal inhibitory concentration (MIC) of tRa and tRb against the Gram positive *Staphylococcus aureus* (ATCC 25,923) and the Gram negative *Escherichia coli* and *Acinetobacter baumannii*. were determined in polystyrene microtiter plates, adding 30 µl of a bacterial inoculum of 10<sup>6</sup> CFU/ml in Mueller–Hinton broth on each well containing 170 µl of each peptide in two-fold serial dilutions (from 200 to 1.5 µM). Assays were performed in duplicate, with incubation for 24 h at 37 °C. MIC value was considered the lowest peptide concentration that completely inhibited the growth of each bacterial strain.

## Results and discussion

### Structural aspects of tRa and tRb

After synthesis, the two temporin peptides were purified by chromatographic steps (Suppl. Figure 1) and had their amino acid sequence and molecular weight checked by mass spectrometry (values are shown in Table 1).

Predictions of secondary structure for both peptides indicate that tRa might assume a disordered/non-helical conformation in aqueous solution with ~80% residues of tRa

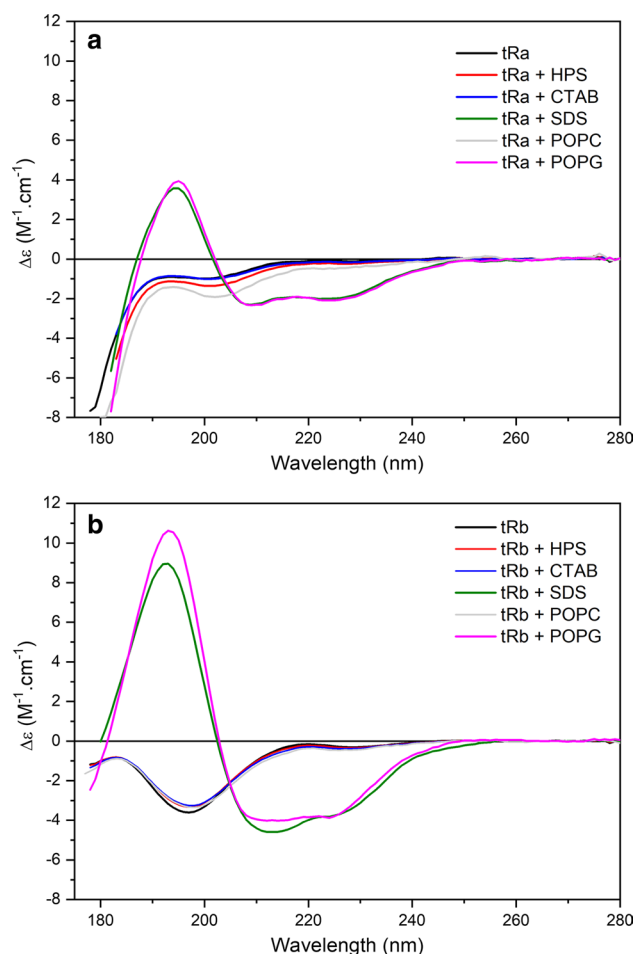


**Fig. 1** SRCD spectroscopy. SRCD spectra of **a** tRa and **b** tRb in aqueous solution (black), and in the presence of 20 mM of HPS (red), CTAB (blue), SDS (green), large unilamellar vesicles of POPC (grey), and POPG (magenta) at a 1/50 P/L molar ratio

in unordered (non-canonical) structure, while for tRb ~70% residues in an extended beta-strand structure were expected (cf. Table 1). The SRCD spectra of both peptides in aqueous solution (Fig. 1) show an intense negative peak at ~198 nm, and an additional small positive peak at ~184 nm. This typical SRCD lineshape is observed in peptides with major disordered content, revealing both peptides, in spite of

**Table 1** Physico-chemical properties of the synthetic peptides

Peptide	Sequence	SSP	MW (Da)	Net charge (pH 7)	<H> <sup>a</sup>	<μH> <sup>b</sup>
tRa	FLKPLFNAALKLLP	ccccccccceec	1584.0	+3	0.826	0.509
tRb	FLPVLAGVLSRA	ccceeeeeeec	1241.5	+2	0.802	0.478

<sup>a</sup>hydrophobicity

<sup>b</sup>hydrophobic moment calculated using HeliQuest (Gautier et al. 2008)

SSP, secondary structure prediction, using GOR4 (Combet et al. 2000), where c stands for disordered and e stands for extended beta



the beta-strand prediction of secondary structure for tRb, assume a disordered, i.e., non-canonical conformation (Wallace 2009; Kumagai et al. 2017) in aqueous solution. The short size chain, the charged and proline residue content in both peptides are features that enable such peptides to assume a disordered state.

However, considering only short range interactions, the predictions of the helical behavior of monomeric peptides give a percentage of helix of 93% and 40% to tRa and tRb, respectively. Both helices also are predicted to form amphipathic structures, with one polar (and positively charged) face and one non-polar side (cf. Supplementary Fig. 2). In fact, disorder-to-helix transitions were observed in the secondary structure of both peptides when TFE was added to the solution (50 and 100%). The SRCD spectra of the peptides changed to show two minima at 222 nm and 208 nm and one positive maximum at 192 nm (Supplementary Fig. 2). The bands assigned to the helix in tRb have higher magnitudes than that seen in the SRCD spectrum of tRa, suggesting that the helical content in the former is higher than in the latter. All the spectral changes observed might be attributed to the displacement and removal of water molecules from the vicinity of the peptides, making the intrachain interactions more favorable (Luo and Baldwin 1997; Cammers-Goodwin et al. 1996).

In the presence of membrane mimics, no conformational changes were observed in the SRCD spectrum of the two temporin peptides when incubated with micelles composed either of zwitterionic (HPS) or positively-charged (CTAB) surfactants. However, the induction of a helix was observed when a negatively charged surfactant (SDS) was used for both tRa and tRb. Similarly, when large unilamellar vesicles composed of the zwitterionic POPC were used, no significant conformational changes were observed in the SRCD spectra of either tRa or tRb. However, in the presence of the negative charge vesicles (POPG), the bands corresponding to the unordered content of the peptides were replaced by those indicating an  $\alpha$ -helix (Fig. 1): the two minima at 222 nm and 208 nm and the positive maximum at 192 nm (Wallace 2009), suggesting the peptide structuring in the vesicles might be dependent on the net surface charge density.

As the binding of both temporins to vesicles of POPG resulted in the induction of a helix structure, we have investigated the orientation of this helix in stacked POPG bilayers CD, since the oriented CD spectroscopy method can be used to estimate the orientation of an  $\alpha$ -helical peptide with respect to the membrane normal. The OCD spectrum of tRa in POPG bilayers (Fig. 2b) has the 208 nm peak more pronounced than the band at 222 nm, which is an evidence for peptide orientation parallel to the plane of the lipid bilayers, i.e., in the surface-bound state (S-state) (Bürck et al. 2016). This orientation was observed for tRa in the entire P/L molar ratio range used, with no realignment of the peptide (or only

a slight re-alignment to a more tilted state when higher P/L molar ratios were used, but presenting all spectra very close to the S-state). When using P/L molar ratios below than 1/50, the OCD spectra obtained would give a very tiny signal (close to background absorption), making clear spectral analysis not possible.

Surprisingly, the OCD spectra of tRa in oriented lipid bilayers of POPC (Fig. 2a) show the peptide assumes also a helix structure when partitioned into this membrane model. All OCD spectra taken have a pronounced negative peak around 208 nm, clearly suggesting that tRa orientation is in the S-state for the entire P/L molar ratio used, indicating tRa does not have a high tendency to re-align in POPC-oriented lipid bilayers either.

In addition, we have conducted SR-OCD experiments with the phospholipids of thinner hydrophobic thickness DOcPC, DDPC, and DLPC, to check whether the tRa helix could align in a different orientation than the S-state, possibly with the peptide spanning the membrane. The short length of the helically folded peptides could only span the thinner membranes (DOcPC and may be DDPC) but not the DLPC, POPC or POPG ones. Once again, the SR-OCD spectra showed tRa is mostly in the S-state (Fig. 3a), with only a slight re-alignment of the peptide at higher peptide concentration (P/L 1:12.5 vs. 1:50) for DLPC and DDPC lipids. At the thinnest hydrophobic thickness bilayers used (DOcPC), it was possible to note a more significant peptide tilt (see P/L 1:12.5 compared with DLPC and DDPC). However, tRa assumes only a tilted state (T-state), and not a clearly inserted state (I-state) (Bürck et al. 2016), even for this “thin” membrane model. For P/L at 1:50 molar ratio in DOcPC, only tiny signals were obtained, hampering the processing of the data reasonably, i.e. the signal of the pure lipid was close to the signal peptide + lipid.

Taking these evidences together, one might suggest that tRa most probably lyses the bacterial membrane using the carpet mechanism, since the peptide stays in the S-state even when a very thin membrane (where it theoretically could span the membrane) is used.

Although conformational changes of tRa peptide in presence of the zwitterionic PC vesicles in aqueous solution had not been observed, the different degree of hydration between the large unilamellar vesicles and the oriented bilayers may be responsible to promote differences in the insertion of the AMP in such model membranes. Similar behavior was described earlier for the antimicrobial peptide Plantaricin-149 (Kumagai et al. 2019), which in the presence of POPC vesicles in aqueous solution presented no conformational changes on its disordered structure, but Pln149 assumed a helix structure when facing the oriented lipid bilayers of POPC, showing the first evidences of peptide interactions with the zwitterionic phospholipid (Fernandez et al. 2013). Moreover, similar to what occurs to tRa,

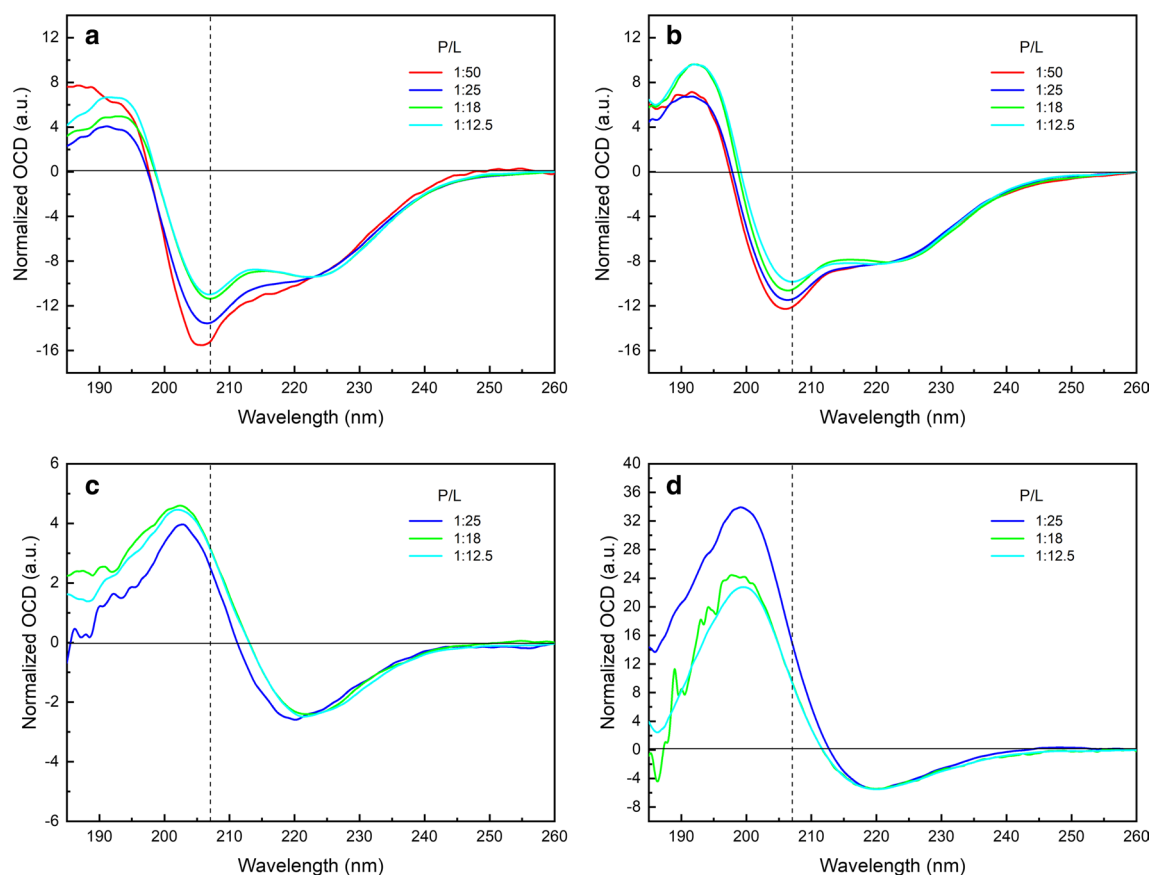


**Fig. 2** Synchrotron radiation oriented circular dichroism spectroscopy. SR-OCD spectra of tRa as a function of P/L molar ratio in **a** POPC or **b** POPG oriented bilayers. SR-OCD spectra of tRb in **c**

POPC or **d** POPG oriented bilayers. All spectra were normalized to the sample of P/L 1:25, using the 220 nm peak

the binding of the antimicrobial peptide to the zwitterionic model might also be modulated by the membrane curvature, as the lipid bilayers used in the OCD assays are planar.

To our surprise, in all the assays conducted to deposit tRb in POPC and POPG oriented bilayers, a clear  $\beta$ -sheet conformation was observed in the SR-OCD spectra (Fig. 2c and 2d). Similar spectra were also observed for tRb in the thinner DLPC, DDPC and DOPC membranes indicating this peptide has a high tendency to aggregate in such systems, no matter what lipid or which P/L molar ratio used (Fig. 3 b). This limitation might also be attributed to any reconstitution problem of the peptide in the bilayers, since the small signal could be due to the very short peptide.

Both alpha-helix and beta sheet conformations have been suggested for other temporin peptides (Mahalka and Kinnunen 2009) although strong evidence for this has been lacking. However, the formation of beta sheets for tRb observed in the OCD samples might be rather an artifact of the OCD hydration conditions than a mechanistically relevant structural transition (same effect have already been observed for the helical antimicrobial peptide MAP (Wadhwani et al. 2008). The absent (or only diminutive) "free water phase"

in OCD sample forces the tRb molecules to partition into the hydrated bilayer. As high P/L ratios (P/L 1:25 up to 1:12.5) had to be used to get reasonable OCD signals, at these high peptide concentration tRb has a distinct tendency to aggregate. Nevertheless, we can conclude that in contrast to tRa at high peptide concentrations in oriented model membranes tRb has a high tendency to aggregate into beta sheets.

### Surface properties of temporin-Ra and temporin-Rb

The peptide tRa presented no adsorption onto a bare air/water interface, presenting surface pressure value of zero throughout the measured time (Fig. 4a). The surface tension value expected for pure water ( $\sim 72.8$  mN/m) was also checked during the entire measurement. The peptide tRb, however, was surface active, migrating from the aqueous subphase to air/water interface, causing changes in the surface pressure value to  $\sim 25$  mN/m.

No peptide adsorption was observed for tRa (up to  $40 \mu\text{M}$ ) when the POPC monolayer was spread onto the air/water interface, suggesting this peptide was not able to adsorb at the zwitterionic surface (Fig. 4b). The peptide tRb,

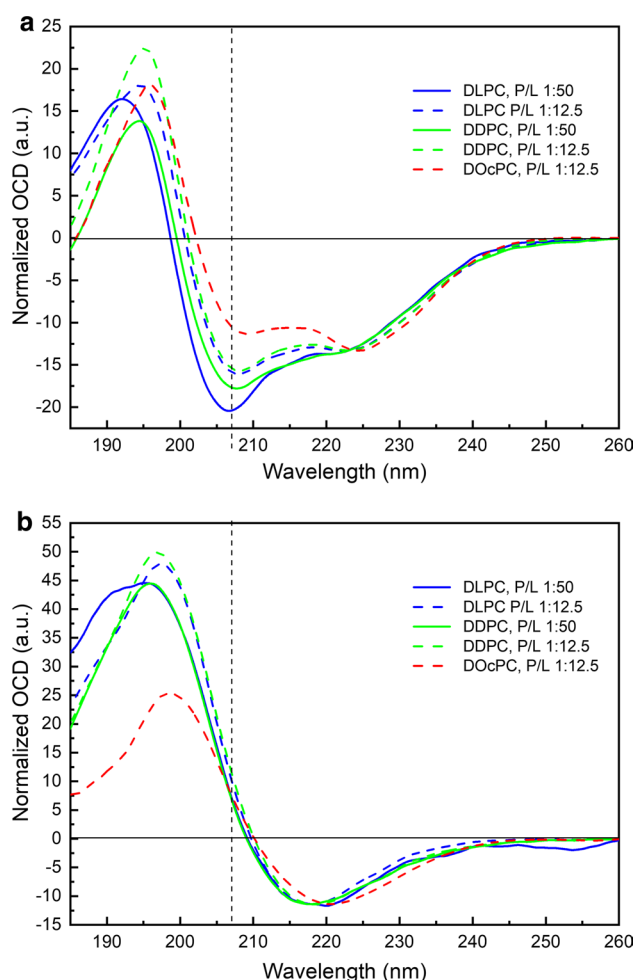


**Fig. 3** Synchrotron radiation oriented circular dichroism spectroscopy. SR-OCD spectra of **a** tRa and **b** tRb as a function of P/L molar ratio in DOcPC, DDPC, and DLPC oriented bilayers (spectra were normalized to the sample of P/L 1:25, using the 220 nm peak)

however, was able to bind the POPC monolayer and weakly disturb lipid packing, causing lateral pressure changes of  $\sim 8$  mN/m (for  $40 \mu\text{M}$  of tRb in subphase).

More significant surface pressure changes were noted by the adsorption of both tRa and tRb onto the POPG monolayer (Fig. 4b). The peptides adsorbed onto the negatively charged lipid surface as a function of the peptide concentration in subphase, in a very similar way. At the highest peptide concentrations used ( $20\text{--}40 \mu\text{M}$ ), however, it seems that adsorption has reached a limit, and surface pressure changes are of  $\sim 15$  mN/m.

The adsorption of tRa and tRb on POPG monolayers were higher when lipid was loosely packed at the interface. As lipid packing density was increased, peptide adsorption reduced significantly as seen in Fig. 4 c. The maximum insertion pressures (MIP) determined for tRa and tRb in POPG monolayers were of  $\sim 31$  mN/m and  $\sim 33$  mN/m, respectively. Such values are within the range estimated for

the lateral pressure of a biological membrane ( $30\text{--}35$  mN/m) (Marsh 1996), indicating both peptides are likely to be bound into biological membranes with a negative surface charge density.

### Biological activity on human erythrocytes and bacterial cells

The results of the hemolytic assays with tRa and tRb presented in Fig. 5, showed that both peptides present low toxicity to human red blood cells, with no hemolysis being detected for both AMPs at peptide concentrations up to  $125 \mu\text{g/mL}$ . At  $250 \mu\text{g/mL}$ , tRa promoted no hemolysis, whilst tRb presented only moderated ( $\sim 10\%$ ) lytic action on red blood cells. Such findings are in close agreement with the lack of interaction observed for both peptides when zwitterionic model membranes in solution are used. The lipid composition of the cell membrane of human red blood cells is mainly composed of zwitterionic phospholipids, such as PC and/or phosphatidyl ethanolamines (PE) lipids (Zaslhoff 2002).

Temporins usually have a relatively narrow spectrum of activity, mainly focused against Gram-positive bacteria. Only a few members of this group have the ability to display a wider spectrum including Gram-negative bacteria and yeasts. As shown in Table 2, in agreement to that, the strains of *E. coli* and *A. baumannii* were weakly inhibited by the action of tRa and tRb presenting high MIC values ( $\sim 160\text{--}300 \mu\text{g/mL}$ ), that can be attributed to the low affinity of these AMPs to the mainly zwitterionic lipid composition of Gram negative bacteria. Moreover, the MIC values determined for tRa and tRb to inhibit the Gram-positive *S. aureus* was of  $\sim 8$  and  $20 \mu\text{g/mL}$ , respectively, which are in close agreement with the interaction of the peptides and the negatively charged model membranes previously observed.

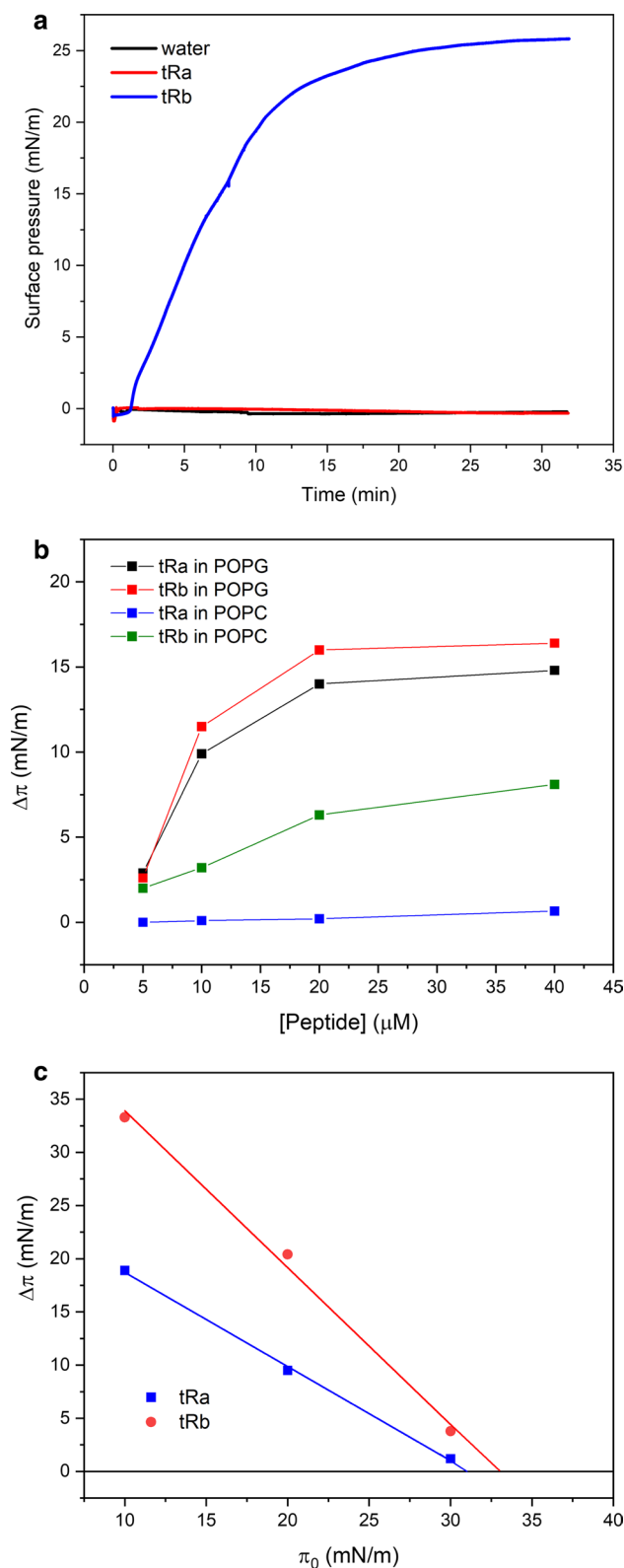
### Conclusions

Several peptide-membrane interactions are known to guide and modulate the activity of the linear cationic AMPs. In this study, the binding of two membrane-active peptides found in the skin of the *Rana ridibunda* was investigated using different model membranes and cells. The binding of these two peptides to the cell membrane depends on an initial electrostatic attraction between the peptides and the negatively charged phospholipids in the membrane surface. Both tRa and tRb are attracted to the surface of the negatively charged phospholipids; they accumulate at the lipid-air interface, and adopt an alpha-helix structure when bound to the lipid surface. At this stage, the peptides are able to interact with the phospholipid headgroups. The helix in tRa adopts an orientation

**Fig. 4** Surface properties. **a** Surface activity of tRa and tRb (40  $\mu\text{M}$ ) in aqueous solution on bare air–water interface. **b** Surface pressure changes caused by the adsorption of tRa and tRb (from 5 to 40  $\mu\text{M}$ ) onto POPG and POPC monolayers. **c** Determination of the maximum insertion pressure (MIP) for tRa and tRb in POPG monolayers. Lipid monolayers were formed with different initial lateral pressure ( $\pi_0$ ). Then, each peptide was injected into the aqueous subphase and the changes in surface pressure ( $\Delta\pi$ ) induced by peptide adsorption were monitored

parallel to the membrane surface, and remains in the “S-state” no matter what lipid (zwitterionic or negatively charged) or P/L molar ratio is used. The peptide tRb can not be reconstituted in stacked lipid bilayers, showing a high tendency to aggregate in  $\beta$ -sheet conformation in such system, but was shown to be surface active and to bind (in minor extent) to zwitterionic lipid surfaces.

The electrostatic attraction modulates the efficiency of peptide binding for both temporin peptides, increases membrane surface lateral pressure and can culminate with the disruption of the model membrane. Taken together, the results suggest the carpet-like model as the mechanism of action for tRa in the lipid systems, since no peptide insertion into the hydrophobic core of the membrane was seen. The knowledge of the membrane binding details for both tRa and tRb are quite useful, and, especially due to their small size and simple amino acid composition, is also attractive for the development of new classes of peptide-based anti-infective drugs.





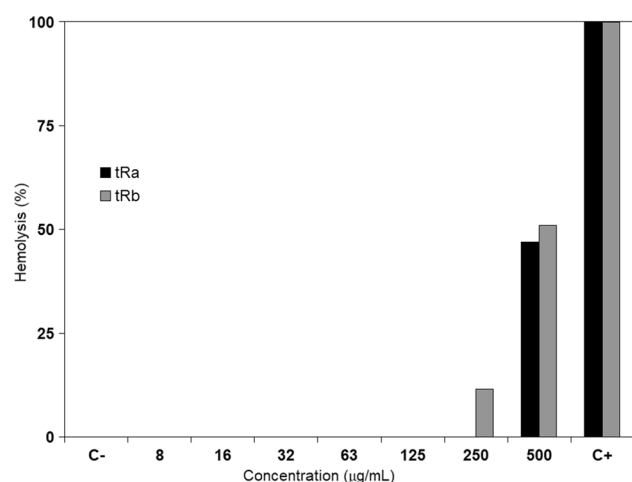


**Fig. 5** Hemolytic assay. Lytic activity of tRa and tRb on red blood cells

**Table 2** MIC for tRa and tRb on bacterial strains

MIC (µg/mL)		
Bacteria	Temporin Ra	Temporin Rb
<i>Staphylococcus aureus</i>	7.76	19.8
<i>Escherichia coli</i>	317	248
<i>Acinetobacter baumannii</i>	158	248

**Supplementary Information** The online version contains supplementary material available at <https://doi.org/10.1007/s00249-022-01615-y>.

**Acknowledgements** This work was supported by grants 2018/19546-7 from Sao Paulo Research Foundation (FAPESP) (to JLSL). We thank beamtime grants on ASTRID2 synchrotron (to JLSL) and access to AU-CD beamline. We acknowledge the KIT light source for provision of instruments at the beamline UV-CD12 of the Institute of Biological Interfaces (IBG2) and we would like to thank the Institute for Beam Physics and Technology (IBPT) for the operation of the storage ring, the Karlsruhe Research Accelerator (KARA).

**Funding** FAPESP, 2018/19546-7, Jose LS Lopes.

## References

- Anthis NJ, Clore GM (2013) Sequence-specific determination of protein and peptide concentrations by absorbance at 205 nm. *Protein Sci* 22(6):851–858
- Asoodeh A, Zardini HZ, Chamani J (2012) Identification and characterization of two novel antimicrobial peptides, temporin-Ra and temporin-Rb, from skin secretions of the marsh frog (*Rana ridibunda*). *J Pept Sci* 18(1):10–16. <https://doi.org/10.1002/psc.1409>
- Bürck J, Roth S, Wadhwani P, Afonin S, Kanithasen N, Strandberg E, Ulrich AS (2008) Conformation and membrane orientation of amphiphilic helical peptides by oriented circular dichroism.

*Biophys J* 95(8):3872–3881. <https://doi.org/10.1529/biophysj.108.136085>

- Bürck J, Wadhwani P, Ulrich FS, AS, (2016) Oriented circular dichroism: a method to characterize membrane-active peptides in oriented lipid bilayers. *Acc Chem Res* 49:184–192
- Cammers-Goodwin A, Allen TJ, Oslick SL, McClure KF, Lee JH, Kemp DS (1996) Mechanism of stabilization of helical conformations of polypeptides by water containing trifluoroethanol. *J Am Chem Soc* 118:3082–3090
- Combet C, Blanchet C, Geourjon C, Deléage G (2000) NPS@: network protein sequence analysis. *TIBS* 25(3):147–150
- Demori I, Rashed ZE, Corradino V, Catalano A, Rovegno L, Queirolo L, Salvidio S, Biggi E, Russo MZ, Canesi L, Catenazzi A, Grasselli E (2019) Peptides for skin protection and healing in amphibians. *Molecules* 24(2):347. <https://doi.org/10.3390/molecules24020347>
- Fernandez DI, Sani MA, Miles AJ, Wallace BA, Separovic F (2013) Membrane defects enhance the interaction of antimicrobial peptides, aurein 1.2 versus caerin 1.1. *Biochim Biophys Acta* 1828:1863–1872
- Gautier R, Douguet D, Antony B, Drin G (2008) Heliquet: a web server to screen sequences with specific  $\alpha$ -helical properties. *Bioinformatics* 24(18):2101–2102
- Helbing CC, Hammond SA, Jackman SH, Houston S, Warren RL, Cameron CE, Birol I (2019) Antimicrobial peptides from *Rana [Lithobates] catesbeiana*: gene structure and bioinformatic identification of novel forms from tadpoles. *Sci Rep* 9:1529. <https://doi.org/10.1038/s41598-018-38442-1>
- Hoskin DW, Ramamoorthy A (2008) Studies on anticancer activities of antimicrobial peptides. *Biochim Biophys Acta* 1778(2):357–375
- Jenssen H, Hamill P, Hancock REW (2006) Peptide antimicrobial agents. *Clin Microbiol Rev* 19(3):491–511. <https://doi.org/10.1128/CMR.00056-05>
- Kaiser E, Collescott RL, Bossinger CD, Cook PI (1970) Color test for detection of free terminal amino groups in the solid-phase synthesis of peptides. *Anal Biochem* 34:595–598
- Kim MK, Kang NH, Ko SJ, Park J, Park E, Shin DW, Kim SH, Lee SA, Lee JI, Leehá EG, Jeon SH, Park Y, SH (2018) Antibacterial and antibiofilm activity and mode of action of magainin 2 against drug-resistant *Acinetobacter baumannii*. *Int J Mol Sci* 19(10):3041. <https://doi.org/10.3390/ijms19103041>
- Kumagai PS, DeMarco R, Lopes JLS (2017) Advantages of synchrotron radiation circular dichroism spectroscopy to study intrinsically disordered proteins. *Eur Biophys J* 46(7):599–606. <https://doi.org/10.1007/s00249-017-1202-1>
- Kumagai PS, Sousa VK, Donato M, Itri R, Beltrami LM, Araujo APU, Buerck J, Wallace BA, Lopes JLS (2019) Unveiling the binding and orientation of the antimicrobial peptide Plantaricin 149 in zwitterionic and negatively charged membranes. *Eur Biophys J* 48(7):621–633
- Kumar P, Kizhakkedathu JN, Straus SK (2018) Antimicrobial peptides: diversity, mechanism of action and strategies to improve the activity and biocompatibility in vivo. *Biomolecules* 8(1):4. <https://doi.org/10.3390/biom8010004>
- Lopes JLS, Gómará MJ, Haro IV, Tonarelli GG, Beltrami LM (2013) Contribution of the Tyr-1 in Plantaricin149a to disrupt phospholipids model membranes. *Int J Mol Sci* 14(6):12313–12328
- Luo P, Baldwin RL (1997) Mechanism of helix induction by trifluoroethanol: a framework for extrapolating the helix-forming properties of peptides from trifluoroethanol/water mixtures back to water. *Biochemistry* 36:8413–8421
- Mahalka AK, Kinnunen PKJ (2009) Binding of amphipathic helical antimicrobial peptides to lipid membranes: Lessons from temporins B and L. *Biochim Biophys Acta* 1788:1600–1609

- Mangoni ML, Grazia AD, Cappiello F, Casciaro B, Luca V (2016) Naturally occurring peptides from *Rana temporaria*: Antimicrobial properties and more. *Curr Top Med Chem* 16(1):54–64
- Marsh D (1996) Lateral pressure in membranes. *Biochim Biophys Acta* 1286:183–223
- Miles AJ, Wallace BA (2018) CDtoolX, a downloadable software package for processing and analyses of circular dichroism spectroscopic data. *Protein Sci* 27(9):1717–1722. <https://doi.org/10.1002/pro.3474>
- Mishra B, Reiling S, Zarena D, Wang G (2017) Host defense antimicrobial peptides as antibiotics: design and application strategies. *Curr Opin Chem Biol* 38:87–96. <https://doi.org/10.1016/j.cbpa.2017.03.014>
- Muñoz V, Serrano L (1997) Development of the multiple sequence approximation within the Agadir model of  $\alpha$ -helix formation. Comparison with Zimm-Bragg and Lifson-Roig formalisms. *Biopolymers* 41:495–509
- Oger PC, Piesse C, Ladram A, Humblot E (2019) Engineering of antimicrobial surfaces by using Temporin analogs to tune the biocidal/antiadhesive effect. *Molecules* 24(4):814. <https://doi.org/10.3390/molecules24040814>
- Rinaldi AC, Mangoni ML, Rufo A, Luzi C, Barra D, Zhao H, Kinunnen PK, Bozzi A, Di Giulio A, Simmaco M (2002) Temporin L: antimicrobial, haemolytic and cytotoxic activities, and effects on membrane permeabilization in lipid vesicles. *Biochem J* 368:91–100
- Rinaldi AC, Conlon JM (2016) Temporins. *Handbook of Biologically Active Peptides* (Second Edition).
- Roy M, Lebeau L, Chessa C, Damour A, Ladram A, Oury B, Boutolleau D, Bodet C, Lévêque N (2019) Comparison of anti-viral activity of frog skin antimicrobial peptides Temporin-Sha and [K<sup>3</sup>]SHA to LL-37 and Temporin-Tb against herpes simplex virus type 1. *Viruses* 11(1):77. <https://doi.org/10.3390/v11010077>
- Varga JFA, Bui-Marinis MP, Katzenback BA (2018) Frog skin innate immune defences: sensing and surviving pathogens. *Front Immunol* 9:3128. <https://doi.org/10.3389/fimmu.2018.03128>
- Wadhwani P, Burck J, Strandberg E, Mink C, Afonin S, Ulrich AS (2008) Using a sterically restrictive amino acid as a 19F NMR label to monitor and to control peptide aggregation in membranes. *J Am Chem Soc* 130(49):16515–16517
- Wallace BA (2009) Protein characterisation by synchrotron radiation circular dichroism spectroscopy. *Q Rev Biophys* 42:317–370
- Zairi A, Tangy F, Bouassida K, Hani K (2009) Dermaseptins and magainins: antimicrobial peptides from frogs' skin - New sources for a promising spermicides microbicides—a mini review. *J Biomed Biotechnol* 2009:452567. <https://doi.org/10.1155/2009/452567>
- Zasloff M (2002) Antimicrobial peptides of multicellular organisms. *Nature* 415:389–395

**Publisher's Note** Springer Nature remains neutral with regard to jurisdictional claims in published maps and institutional affiliations.

Springer Nature or its licensor holds exclusive rights to this article under a publishing agreement with the author(s) or other rightsholder(s); author self-archiving of the accepted manuscript version of this article is solely governed by the terms of such publishing agreement and applicable law.